A STUDY OF A DIELECTRIC BACKED RESONANT SLOT ANTENNA

Uwe Siegfried Kahre

NAVAL POSTGRADUATE SCHOOL
Monterey, California

THESIS

A STUDY OF A DIELECTRIC BACKED RESONANT SLOT ANTENNA

by

Uwe Siegfried Kahre

December 1975

Thesis Advisor: J. B. Knorr

Approved for public release; distribution unlimited.

SECURITY CLASSIFICATION OF THIS PAGE *(When Data Entered)*

REPORT DOCUMENTATION PAGE

READ INSTRUCTIONS BEFORE COMPLETING FORM

1. REPORT NUMBER	2. GOVT ACCESSION NO. / 3. RECIPIENT'S CATALOG NUMBER
4. TITLE *(and Subtitle)*: A Study of a Dielectric Backed Resonant Slot Antenna	5. TYPE OF REPORT & PERIOD COVERED: Master's Thesis December 1975
	6. PERFORMING ORG. REPORT NUMBER
7. AUTHOR(s): Uwe Siegfried Kahre	8. CONTRACT OR GRANT NUMBER(s)
9. PERFORMING ORGANIZATION NAME AND ADDRESS: Naval Postgraduate School, Monterey, California 93940	10. PROGRAM ELEMENT, PROJECT, TASK AREA & WORK UNIT NUMBERS
11. CONTROLLING OFFICE NAME AND ADDRESS: Naval Postgraduate School, Monterey, California 93940	12. REPORT DATE: December 1975
	13. NUMBER OF PAGES: 52
14. MONITORING AGENCY NAME & ADDRESS *(if different from Controlling Office)*	15. SECURITY CLASS. *(of this report)*: UNCLASSIFIED
	15a. DECLASSIFICATION/DOWNGRADING SCHEDULE

16. DISTRIBUTION STATEMENT *(of this Report)*

Approved for public release; distribution unlimited

17. DISTRIBUTION STATEMENT *(of the abstract entered in Block 20, if different from Report)*

18. SUPPLEMENTARY NOTES

19. KEY WORDS *(Continue on reverse side if necessary and identify by block number)*

Slot Antenna
Dielectric Backed
Radiation Resistance, Radiation Patterns

20. ABSTRACT *(Continue on reverse side if necessary and identify by block number)*

This thesis describes a study of a dielectric backed resonant slot antenna, E-field and radiation resistance were calculated and compared with measurements. Special effort was devoted to impedance matching between the transition from the coaxial cable to the slot. The effect of this matching on radiation patterns was discussed and the bandwidth of the antenna measured.

DD FORM 1 JAN 73 1473 EDITION OF 1 NOV 65 IS OBSOLETE
S/N 0102-014-6601 |
(Page 1)

SECURITY CLASSIFICATION OF THIS PAGE *(When Data Entered)*

A Study of a Dielectric Backed Resonant Slot Antenna

by

Uwe Siegfried Kahre
Kapitänleutnant, Federal German Navy

Submitted in partial fulfillment of the
requirements for the degree of

MASTER OF SCIENCE IN ELECTRICAL ENGINEERING

from the

NAVAL POSTGRADUATE SCHOOL

December 1975

ABSTRACT

This thesis describes a study of a dielectric backed resonant slot antenna. E-field and radiation resistance were calculated and compared with measurements. Special effort was devoted to impedance matching between the transition from the coaxial cable to the slot. The effect of this matching on radiation patterns was discussed and the bandwidth of the antenna measured.

TABLE OF CONTENTS

LIST OF FIGURES

ACKNOWLEDGEMENT

I am very much obliged to the Federal German Navy for giving me the opportunity to complete my graduate education.

I gratefully acknowledge my indebtness to my thesis advisor for his continuous aid.

1.0 INTRODUCTION

The study of resonant slot antenna on a dielectric backed substrate, as shown in figure 1.0/1, can be of prime importance where no outstanding antenna structure is wanted. An example where this might be necessary is an aircraft. A dielectric backed resonant slot can also be used for radiating into a waveguide.

The important characteristics of an antenna are radiation resistance and field patterns. These are studied first theoretically. In this study it was found in theory and in practice that a resonant slot antenna presents a high radiation resistance and thus a high input impedance as seen from a coaxial transmission line. It is, however, possible to obtain a better match between the microstrip and the slot. A matching by positioning the microstrip on certain locations with respect to the slot can roughly be predicted, as will be shown. The radiation patterns are similar to the dipole pattern, the similarity depending somewhat on the position of the microstrip as indicated above.

In determining the slot dimension for a given frequency Ref. 2,4 and 5 were of prime importance.

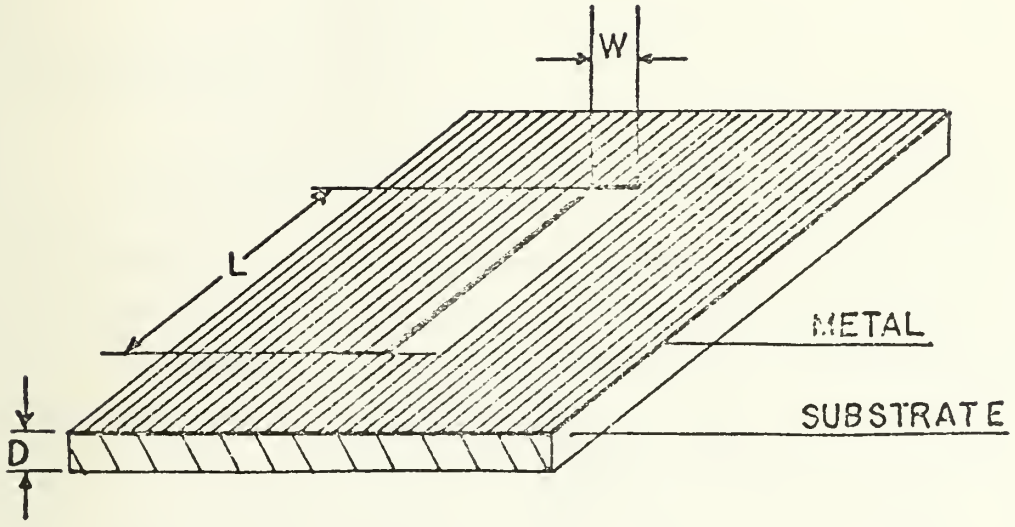

Figure 1.0/1 Dielectric Backed Slot Antenna.

2.0 CALCULATION OF THE ELECTROMAGNETIC FIELD

When calculating the electromagnetic field, the far field approximation will be used. The slot is centered as shown in figure 2.1/1a.

2.1 ASSUMPTIONS

The assumptions used are:

a) Infinite ground plane.
b) The conducting plate represents a perfect conductor.
c) The E-field across the slot is sinusoidal.
e) No radiation on dielectric side of the metal.
d) E(x) is uniform.

The sinusoidal E-field is shown in figure 2.1/1b.

2.2 SOLUTION

By assumption (b) the EM-field can be computed from a knowledge of the E-field alone. The E-field across the slot is replaced by an equivalent magnetic current sheet (figure 2.2/2a and b). Now the EM-field to the right is the result of the magnetic surface current $\vec{M}$ and the electric current flowing in the conducting plane. Applying the image principle, the plane and current can be replaced by those of figure 2.2/2d. As $\vec{n} \times \vec{E}=\vec{M}$ over the aperture and $\vec{n} \times \vec{E}=0$ elsewhere, the EM-field to the right is the same for figure 2.2/2a. A general procedure for replacing an electric field by an equivalent magnetic current sheet is contained in Ref. 1 pp. 472-474.

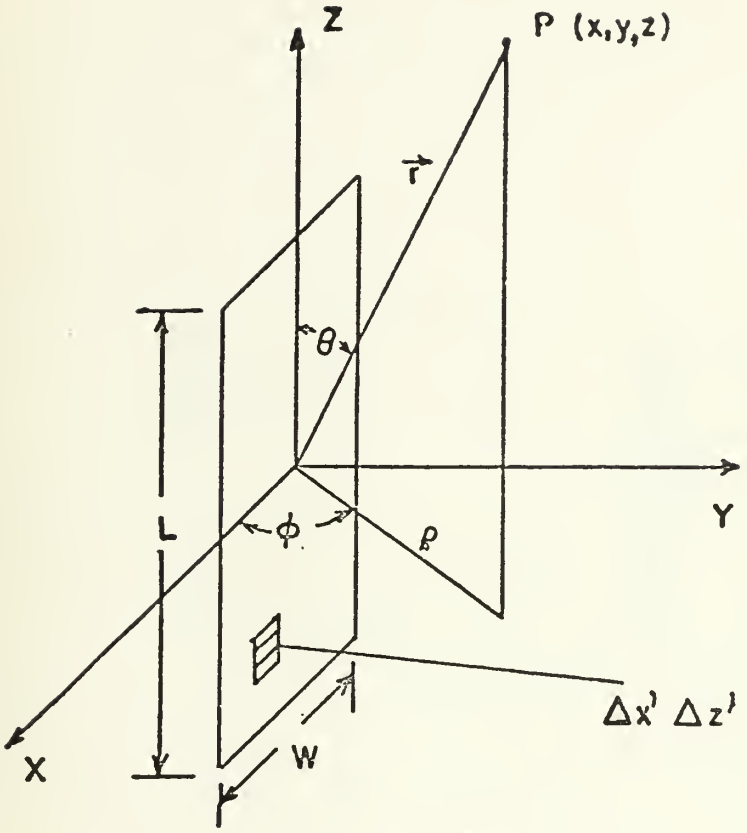

a)

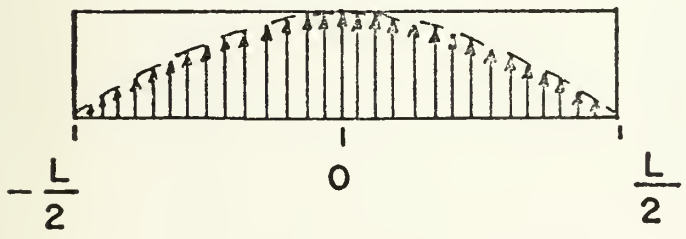

b)

Figure 2.1/1 a) Slot Orientation
b) E-Field Distribution in the Slot

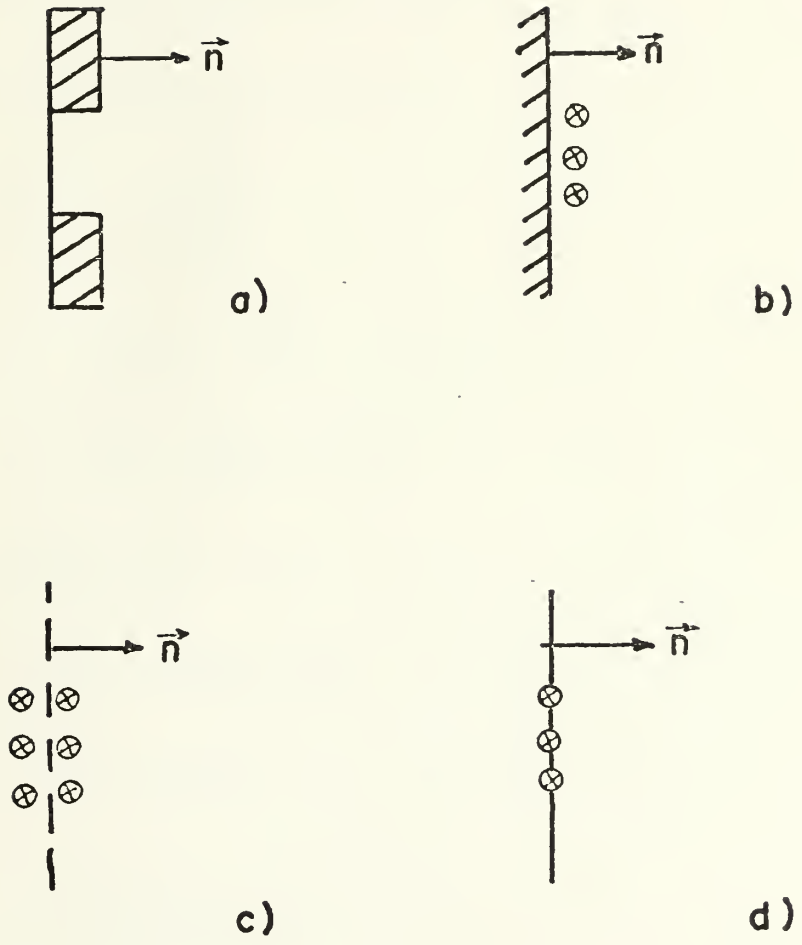

Figure 2.1/2 Replacement of the Electric Field by an Equivalent Current Sheet.

The electric vector potential F will be in the z direction and will have the value

$$F_z = \frac{\epsilon}{4\pi} \int_{-\frac{L}{2}}^{\frac{L}{2}} \int_{-\frac{w}{2}}^{\frac{w}{2}} \frac{M_z(x',z')\, e^{-j\beta|\vec{r}-\vec{r}'|}}{|\vec{r}-\vec{r}'|}\, dx'dz' \quad .$$

For the far field approximation:

$|\vec{r}-\vec{r}'| = r$ in the denominator

$$|\vec{r}-\vec{r}'| = |\vec{r}| - \frac{|\vec{r}'\cdot\vec{r}|}{|\vec{r}|} \quad .$$

where $\vec{r}' = x'\vec{a}_x + z'\vec{a}_z$

$\vec{r} = x\vec{a}_x + y\vec{a}_y + z\vec{a}_z$

thus $\vec{r}'\cdot\vec{r} = xx' + zz'$

$x = r \sin\theta \cos\phi$

$z = r \cos\theta$

$$\frac{\vec{r}'\cdot\vec{r}}{\vec{r}} = x' \sin\theta \cos\phi + z' \cos\theta$$

and $|\vec{r}-\vec{r}'| = r - x' \cos\phi \sin\theta - z' \cos\theta$.

$$F_z = \frac{K_o \varepsilon}{4\pi r} \int_{-\frac{L}{2}}^{\frac{L}{2}} \int_{-\frac{w}{2}}^{\frac{w}{2}} \cos\frac{\pi z'}{L} \exp(-j\beta(r - x'\cos\phi\sin\theta - z'\cos\theta))dx'dz'$$

but $\cos\frac{z'\pi}{L} = 0.5(e^{\frac{j\pi z'}{L}} + e^{\frac{-j\pi z'}{L}})$

$$F_z = \frac{K_o \varepsilon e^{-j\beta r}}{8\pi r} \int_{-\frac{w}{2}}^{\frac{w}{2}} e^{j\beta x'\cos\phi\sin\theta} dx' \left(\int_{-\frac{L}{2}}^{\frac{L}{2}} e^{jz'(\beta\cos\theta+\frac{\pi}{L})} dz' + \int_{-\frac{L}{2}}^{\frac{L}{2}} e^{jz'(\beta\cos\theta-\frac{\pi}{L})} dz'\right)$$

$$\int_{-\frac{L}{2}}^{\frac{L}{2}} e^{jz'(\beta\cos\theta+\frac{\pi}{L})} dz' = -2\cos(\beta\frac{L}{2}\cos\theta)\ (\beta\cos\theta+\frac{\pi}{L})^{-1}$$

$$\int_{-\frac{L}{2}}^{\frac{L}{2}} e^{jz'(\beta\cos\theta-\frac{\pi}{L})} dz' = 2\cos(\beta\frac{L}{2}\cos\theta)\ (\beta\cos\theta-\frac{\pi}{L})^{-1}$$

$$(\beta\cos\theta-\frac{\pi}{L})^{-1} - (\beta\cos\theta+\frac{\pi}{L})^{-1} = \frac{2L\pi}{(L\beta\cos\theta)^2 - \pi^2}$$

Thus the integration over z leads to

$$\frac{4L\pi\cos(\beta\frac{L}{2}\cos\theta)}{(L\beta\cos\theta)^2 - \pi^2} \quad .$$

$$\int_{-\frac{w}{2}}^{\frac{w}{2}} e^{j\beta x'\cos\phi\sin\theta}\, dx' = \frac{2\sin(\beta\frac{w}{2}\cos\phi\sin\theta)}{\beta\cos\phi\sin\theta}$$

$$F_z = K_o \varepsilon L \frac{e^{-j\beta r}}{\beta r} \frac{\sin(\beta\frac{w}{2}\cos\phi\sin\theta)\ \cos(\beta\frac{L}{2}\cos\theta)}{\cos\phi\ \sin\theta\ ((L\beta\cos\theta)^2 - \pi^2)}$$

$$H_\theta = -j\omega F_\theta$$

$$= j\omega F_z \sin\theta$$

and let $\frac{\beta w}{2} = \frac{\pi w}{D}\frac{D}{\lambda}$

$$L\beta = \frac{2L}{\lambda'}\frac{\lambda'}{\lambda}\pi$$

$$H_\theta = \frac{jK_o L}{\eta\pi^2} \frac{e^{-j\beta r}}{r} \frac{\sin(\frac{D}{\lambda}\frac{\pi w}{D}\cos\phi\sin\theta)\ \cos(\frac{\pi L}{\lambda'}\frac{\lambda'}{\lambda}\cos\theta)}{\cos\phi\ ((\frac{2L}{\lambda'}\frac{\lambda'}{\lambda}\cos\theta)^2 - 1)}$$

$$H_\phi = 0$$

The strength of the distant electric field will be

$$E_\phi = -\eta H_\theta$$

$$= \frac{-jK_o L}{\pi^2} \frac{e^{-j\beta r}}{r} \frac{\sin(\frac{D}{\lambda} \frac{\pi W}{D} \cos\phi \sin\theta) \cos(\frac{\pi L}{\lambda'} \frac{\lambda'}{\lambda} \cos\theta)}{\cos\phi((\frac{2L}{\lambda'} \frac{\lambda'}{\lambda} \cos\theta)^2 - 1)}$$

$$E_\theta = 0$$

2.3 DETERMINTION OF CONSTANTS

The constants to be determined are:

independent: ε_r, $\frac{D}{\lambda}$, $\frac{W}{D}$

dependent: $\frac{L}{\lambda'}, \frac{\lambda'}{\lambda}$

Let $\varepsilon_r = 20$

$$\frac{D}{\lambda} = 0.03175$$

$$\frac{W}{D} = 1.0$$

Reference 2 contains results of slot line parameters from which the graphical representation of figure 2.3/1 was taken. From this figure the wavelength ratio is 0.358. The equivalent circuit for a resonant slot is indicated in figure 2.3/2, where the normalized input impedance equals infinity at resonance.

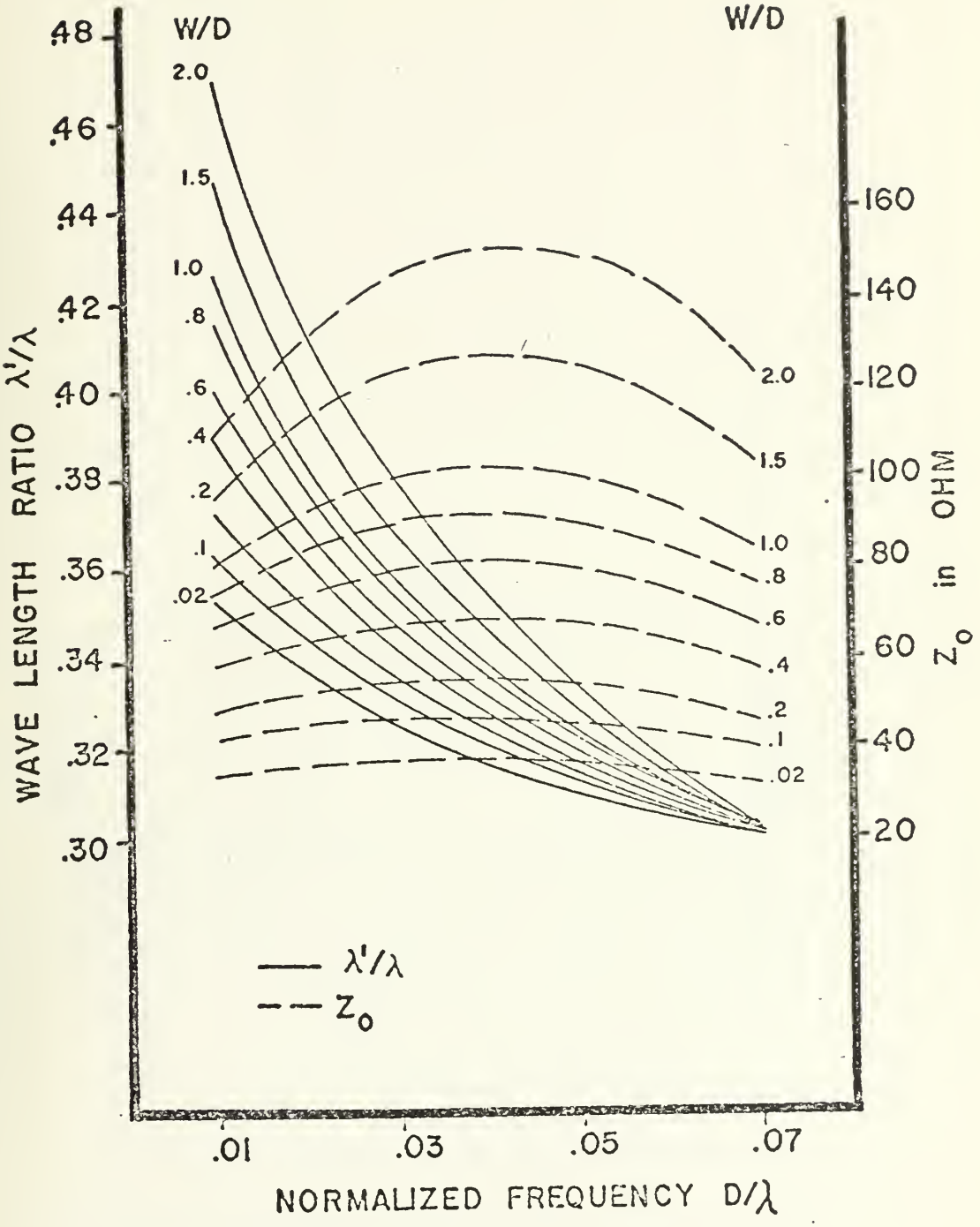

Figure 2.3/1 Dispersion Characteristic and Characteristic Impedance of a Single Slot Line with Relative Dielectric Constant of 20 (Ref. 2).

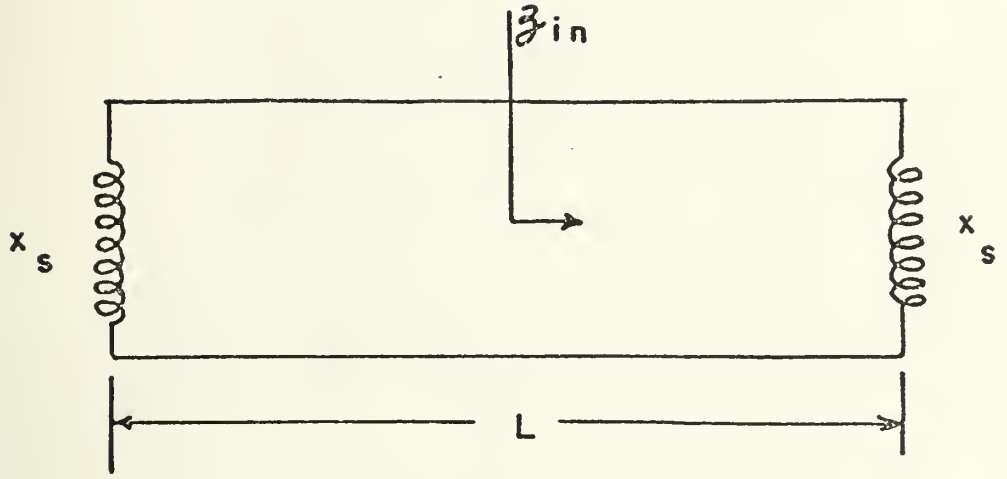

Figure 2.3/2 Equivalent Circuit for a Resonant Slot.

$$z_{in} = \frac{z_r + j\tan\beta L}{1 + jz_r\tan\beta L}$$

$$z_r = jx_s$$

$$x_{in} = \frac{x_s + \tan\beta L}{1 - x_s\tan\beta L}$$

for $x_{in}(\frac{L}{2}) = \infty$

$$1 - x_s\tan\beta\frac{L}{2} = 0$$

$$\beta\frac{L}{2} = \tan^{-1}\frac{1}{x_s}$$

$$\frac{L}{\lambda'} = \frac{1}{\pi}\tan^{-1}\frac{1}{x_s}$$

The normalized reactance for several different dielectric constants vs. the thickness to wavelength ratio was graphically presented by Knorr and Saenz (Ref. 3) from which figure 2.3/3 is shown. The normalized reactance obtained from this figure at a frequency of 3 GHz is 0.38.

A summary of the constants is presented below.

$\varepsilon_r = 20$

$\frac{D}{\lambda} = 0.03175$

$\frac{W}{D} = 1.0$

$\frac{\lambda'}{\lambda} = 0.358$

$\frac{L}{\lambda'} = 0.384$

2.4 PLOT OF THE E-FIELD

The E-field was plotted on the HP 9821A calculator. Three prcgrams were written, the first for a plot E versus Theta for Phi equals ninety degrees. The mathematical expression was obtained by a limiting process:

$$\lim_{\phi \to \frac{\pi}{2}} E = \frac{-jK_o L}{\Pi^2} \frac{e^{-j\beta r}}{r} \frac{(\frac{D}{\lambda} \frac{\pi w}{D} \sin\theta)\ (\cos(\frac{\pi L}{\lambda'} \frac{\lambda'}{\lambda} \cos\theta))}{((\frac{2L}{\lambda'} \frac{\lambda'}{\lambda} \cos\theta)^2 - 1)}$$

$$= \frac{-jK_o L}{\pi^2} \frac{e^{-j\beta r}}{r} \frac{C_1 \sin\theta \cos(C_2 \cos\theta)}{((C_3 \cos\theta)^2 - 1)}$$

This program is contained in appendix A.

The second program is for a plot E versus Theta and is based on the original equation. It can be used for any Phi except Phi equals ninety degrees. The program is presented in appendix B. For a comparison both programs were used to draw a plot on the same paper with a slight difference in Phi. Phi equals 0.0001 in the second program. Both plots are congruent as can be seen in figure 2.3/1. The magnitude plot shows that this pattern is similar to the dipole pattern. The beamwidth equals 82 degrees.

The third prcgram, presented in appendix C, draws a plot E versus Phi, as shown in figure 2.4/2. In order to prove that the plot is nearly half a circle as in the dipole case, three points were checked. As the sine of a small angle equals nearly the angle, the pattern should show almost a half circle which it does.

$$E_\phi = \frac{-jK_oL}{\pi^2} \frac{e^{-j\beta r}}{r} \frac{\sin(C_1 \cos\phi\sin\theta)\cos(C_2 \cos\theta)}{\cos\phi\,((C_3 \cos\theta)^2 - 1)}$$

$$\text{let} \quad \frac{-jK_oL}{\pi^2} \frac{e^{-j\beta r}}{r} = K$$

$$\lim_{\phi\to\frac{\pi}{2}} E_\phi = KC_1$$

$$E_\phi \Big|_{\phi=\pi} = K\sin(-C_1)$$

$$E_\phi \Big|_{\phi=0} = K\sin C_1$$

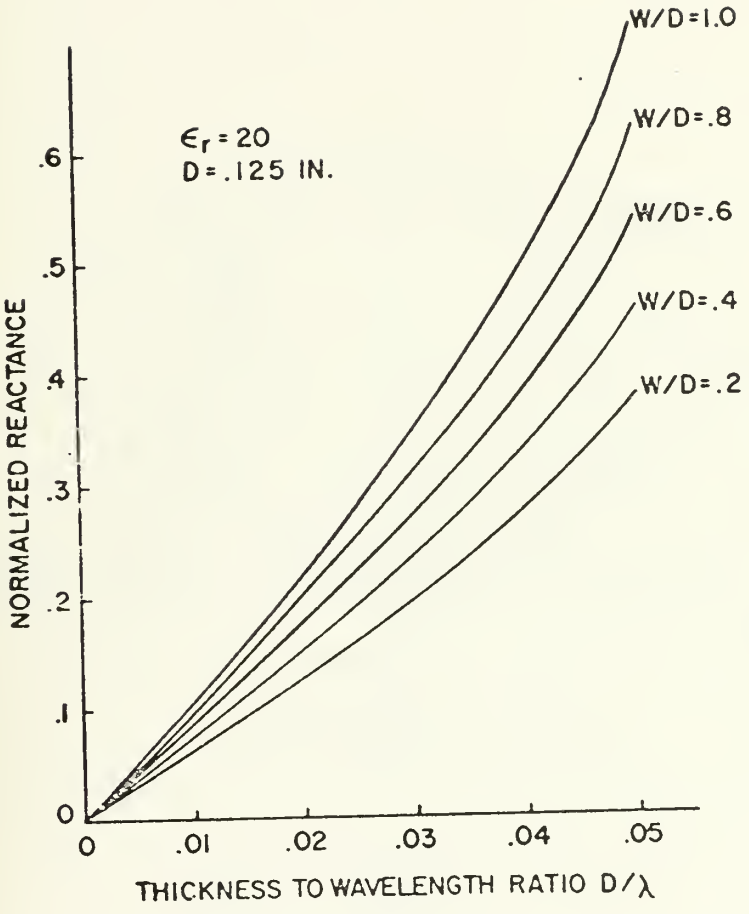

Figure 2.3/3 Normalized Reactance vs. Thickness to Wavelength Ratio (Ref. 3).

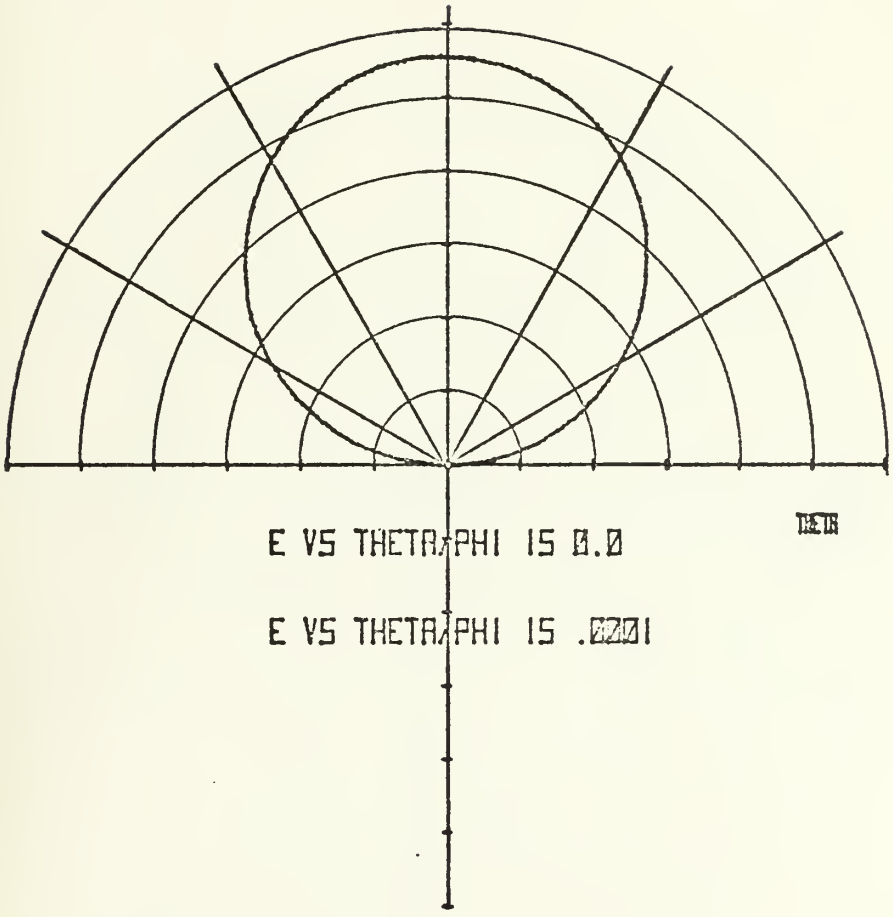

Figure 2.4/1 E-Field Pattern in the Vertical Plane.

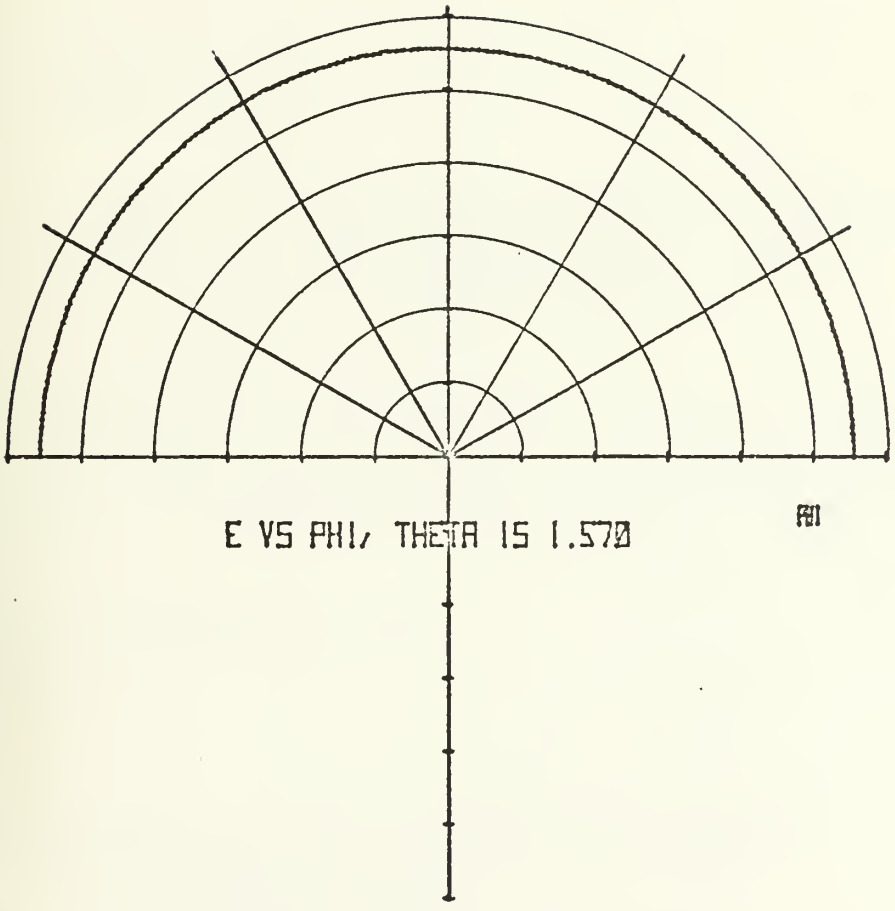

Figure 2.4/2 E-Field Pattern in the Horizontal Plane.

3. EVALUATION OF THE RADIATION CONDUCTANCE

In the last chapter the expression for the electromagnetic field was derived. In spherical coordinates the outward radial power flow of complex power per unit area is

$$P_r = \frac{1}{2} (E_\theta H_\phi^* - E_\phi H_\theta^*)$$

$$E_\theta = H_\phi = 0$$

$$P_r = -\frac{1}{2} E_\phi H_\theta^*$$

$$= \frac{1}{2\eta} \frac{K_o^2 L^2}{\pi^4} \frac{1}{r^2} \frac{\sin^2(\frac{D}{\lambda} \frac{\pi W}{D} \cos\phi\sin\theta) \cos^2(\frac{\pi L}{\lambda'} \frac{\lambda'}{\lambda} \cos\theta)}{\cos^2\phi \ ((\frac{2L}{\lambda'} \frac{\lambda'}{\lambda} \cos\theta)^2 - 1)^2}$$

The total power radiated can be computed by integrating the Poynting vector over half the spherical surface centered at the slot.

$$W = \int_0^\pi \int_0^\pi P_r \, r^2 \sin\theta \, d\phi \, d\theta$$

The problem now is to evaluate the integral.

Let $F = \int_0^\pi \int_0^\pi G(\theta,\phi) \, d\theta \, d\phi$

$$= \frac{\sin\theta \sin^2(C_1 \cos\phi\sin\theta) \cos^2(C_2\cos\theta)}{\cos^2\phi \ ((C_3\cos\theta)^2 - 1)^2}$$

$$C_1 = \frac{D}{\lambda} \frac{\pi W}{D}$$

$$C_2 = \frac{\pi L}{\lambda'} \frac{\lambda'}{\lambda}$$

$$C_3 = \frac{2L}{\lambda'} \frac{\lambda'}{\lambda} = \frac{2}{\pi} C_2$$

There is one singularity at Phi equals 90 degrees.

$$\lim_{\phi \to \frac{\pi}{2}} G(\phi) = K_1 \lim_{\phi \to \frac{\pi}{2}} \frac{\sin^2(K_2 \cos\phi)}{\cos^2\phi}$$

where K_1 and K_2 are some constants.

By l'Hopital's rule

$$= K_1 \lim_{\phi \to \frac{\pi}{2}} \left(K_2^2 \frac{\cos(K_2\cos\phi) \sin\phi \cos(K_2\cos\phi)}{\sin\phi} \right.$$

$$\left. -K_2^2 \frac{\sin(K_2\cos\phi) \sin\phi \sin(K_2\cos\phi)}{\sin\phi} \right.$$

Thus at Phi equals 90 degrees there is a removable singularity. There might be a second singularity when C_3 times the cosine of Theta equals unity. For C_3 less than unity this will not happen. As C_3 equals two times the slotlength over the free space wavelength, which is of a higher value, C_3 is always less than unity. The integral

was evaluated by the trapezoidal rule.

$$\Delta F_{i,j} = G(I-\frac{1}{2},\ J-\frac{1}{2})$$

$$F = \sum_{i=1}^{N} \sum_{j=1}^{N} G(I-\frac{1}{2},\ J-\frac{1}{2})\ \Delta\phi_i\ \Delta\theta_j$$

where $\Delta\phi = \Delta\theta = \frac{\pi}{N}$

$$I-\frac{1}{2} = (i-\frac{1}{2})\ \Delta\phi$$

$$J-\frac{1}{2} = (j-\frac{1}{2})\ \Delta\theta$$

The program for evaluation of the integral is contained in appendix D.

For the evaluation of the conductance, P has to be in the form

$$P = GV^2$$

$$K_o^2 = \frac{4V^2}{W2} \quad \text{and} \quad \frac{K_o^2 L^2}{2\pi^4 \eta} = \frac{2V^2 L^2}{\eta \pi^4 W^2}$$

$$\frac{P}{(\frac{L}{W})^2} = (\frac{F}{60\pi^5})\ V^2$$

F from the numerical integration is 0.41566E-01, which gives a value for the radiation resistance of 23529 ohms.

In this equation the power is inverse proportional to the width. This does not seem to be correct as it should grow with the area.

The integrand of the integral after letting the cosine of Phi and the sine of Theta equal unity is:

$$\frac{\sin^2(\pi\frac{W}{\lambda})\ \cos(\pi\frac{L}{\lambda})}{(\frac{4L^2}{\lambda} - 1)^2} \quad .$$

As the argument of the sine squared term is small, it can be replaced by the angle itself. Thus the width will cancel. The width, however, is still hidden in the constants determined by the design curves.

4. CONSTRUCTION AND FIRST TESTING OF THE SLOT ANTENNA

After the theoretical study an antenna should be built and its performance compared with the theoretical results. The antenna was constructed by etching the slot and a microstrip on a dielectric substrate metallized on both sides.

4.1 THE ETCHING PROCESS

General notes on microwave stripline circuit fabrication are in Ref. 4. The slot antenna dimensions and the substrate used were mainly decided upon in chapter two by determining the constants. The manufacturer's supply substrate has a thickness of 0.125 inches and is metallized on both sides with copper. The dielectric constant is 20 and the size of the board was chosen to be a square of three inches on one side. In order to cut this size one must be careful not to crack the dielectric.

The dimensions of the slot antenna to be etched on one side are 1.374 cm times 0.3175 cm. On the opposite side a microstrip conductor has to be constructed by etching which crosses the slot at right angle and extends one-quarter of a wavelength beyond the slot and similarly, the slot extends about one quarter of a wavelength beyond the microstrip.

The microstrip impedance was chosen to be 50 ohms and the dimension obtained from Ref. 5 is 0.062 inches. A 50 ohm impedance was chosen in order to match the circuit to the HP 8410 S microwave network analyzer for reflection measurements.

For etching the slot and the microstrip it is necessary to have the negative of the slot and the positive of the

microstrip. As the dimensional tolerances are extremely critical in microwave circuits, the preparation of high quality negatives and positives is essential. This is accomplished by using manufactured black adhesive stripes in oversize and having them photoreduced. The percentage of reduction is determined by the available dimensions of the stripes. This work was performed by the Educational Media Department Photographic Laboratory.

The next step in the fabrication process is the photo sensitization of the metal on the substrate. For this, cleanliness of the metal surface is essential. It should be free of grease and any foreign material. This can be achieved by using alcohol or acetone. The surface to be etched must then be uniformly coated by a spray resist in an aerosol can. Immediately after spraying, the substrate has to be dried in a light proof oven at about 140 degrees Farenheit for ten minutes. After spraying, the board must be protected from light until development.

Great care must be taken in positioning the negative and positive properly with respect to each other. This is best done under a microscope. Thereafter, the board is inserted between them and then exposed to ultra violet light for about six minutes on each side. Those areas exposed to the light become hardened, and this layer will protect the metal from the etchant. After exposing, the board is placed in a developer of trichloroethylene solution which removes the unexposed spray resist. The developer solution has to evaporate before the board can be dipped into the etchant for about ten minutes, depending on the thickness of the copper and the quality of the etchant. The final part of the etching process is a control under a microscope for any copper flecks or wrong dimensions.

4.2 FIRST TEST RESULTS

Though having calculated a radiation resistance of about 23000 ohms, it was decided to use a microstrip of an impedance of 50 ohms to measure the reflection coefficient on the HP 8410 S to get a feeling of the accuracy of the calculation.

After the etching process, a connection from coaxial cable to the microstrip was fastened to the board and the normalized input impedance measured. For the measurement of the reflection coefficient, the microwave analyzer has to be calibrated with a short at the input port. When connecting the board, however, the shift in the reference plane must be taken care of which can be calculated by:

$$\theta_{ref} = \theta_{test}$$

$$\frac{2\pi}{\lambda} \Delta l_{ref} = \frac{2\pi}{\lambda'} \Delta l_{test}$$

$$\Delta l_{ref} = \Delta l_{test} \frac{\lambda}{\lambda'}$$

The difference of the test length was measured from the center of the slot to the edge of the board. Taking this shift into account, the normalized input conductance was 0.008 - j0.135. This leads to a radiation resistance of 6250 ohms. As accuracy in that range could not be achieved due to the limitation of the analyzer, this value is an indication of the correctness of the calculation because both numbers are of the same degree of magnetude. The lower value can also be attributed to the fact that radiation from the dielectric side lowers the radiation resistance. The conclusion to be drawn is that the microstrip saw

effectively an open circuit.

4.3 EXPERIMENTS WITH IMPEDANCE MATCHING

As the mismatch of the microstrip to the slot is in the range as the calculation predicted, a power microwave oscillator was thought to be necessary for recording radiation patterns. Having none available at a frequency of 3 GHz, it was decided to redesign the slot for a frequency of 2.25 GHz. The new values of the constants, obtained as outlined in chapter 2.3, are:

$$\varepsilon_r = 20$$

$$\frac{W}{D} = 1$$

$$\frac{D}{\lambda} = 0.0238$$

$$\frac{\lambda'}{\lambda} = 0.376$$

$$\frac{L}{\lambda'} = 0.4172$$

The constants in the computer program of appendix D were changed accordingly. The evaluation of the integral gave 0.023354 which leads to a radiation resistance of 18092 ohms. The three calculator programs of appendix A to C were also changed and the E-field pattern displayed almost exactly the same graphs as in figure 2.4/1 and 2.4/2. Only the beamwidth increased to 84 degrees.

In order to obtain an idea of how the resistance decreases with frequency, a series of seven values was calculated for a constant width to thickness ratio and the

same dielectric constant. This curve is presented in figure 4.3/1.

In figure 2.1/1b the E-field distribution over the slot is indicated. The transmission line has a resistance of 50 ohms, but the radiation resistance was calculated to be about 18000 ohms at 2.25 GHz. For power transfer under better matched conditions, the 50 ohm-line has to lead into a higher resistance. One way to achieve this is to let the 50 ohm microstrip taper off. This has limitations in the production process of the board.

A second possibility is to move the microstrip from the slot-center to the edge. As the voltage was assumed to be a cosine distribution over the slot with the maximum voltage at the center and zero at the edges, the conductance should decrease as:

$$G = G_o \cos^2 \frac{\pi x}{L}$$

where G-zero is the conductance at the slot center. However, this will only be correct as long as one does not reach into the region where the edge effects of the slot become important. The change in the conductance also says that the input resistance should also change with the cosine squared of the same angle.

As a first verification, a series of three boards were etched with the same slot and microstrip dimensions. The microstrip was designed to taper off from its 50 ohm width of 0.157 cm to 0.0275 cm on all three boards. The only difference between the three boards was the position of the microstrip with respect to the slot as set forth in figure 4.3/3. The position angles are 0, 45, 67.5 degrees. The normalized input impedance was then measured on the microwave analyzer and plotted by the WANG 600 calculator, as shown in figure 4.3/3, with the primed conductances

representing the coordinates as given from the calculator. From the data follows:

g(1) = 0.05 - j0.89

g(2) = 0.115 - j1.06

g(3) = 0.175 - j1.0

Thus the input resistance is:

R(1) = 1000 ohm

R(2) = 434 ohm

R(3) = 286 ohm

Based on R(1) of 1000 ohms and the above equation the calculation would predict the values:

R(2) = 500 ohm

R(3) = 146 ohm.

The direction and the magnetude of the resistances is what theory predicts. The difference can be explained mainly by the edge effects of the slot which are not yet sufficiently analyzed to be included into the calculation. There might also be slight differences in the actual position due to the etching process.

The general conclusions to be drawn from the above calculaticns are:

Impedance matching in the microwave region is very difficult. In order to use low powered oscillators, one has to stay in a far lower frequency region.

There are two possibilities for achieving a better impedance match for a given frequency, width to thickness ratio, and dielectric constant: tapering the microstrip and/or positioning it closer to the edge. The first has to be done by cut and try method as this is not yet thoroughly analyzed. The results of the second can roughly be predicted as long as one does not come too close to the edge. There the effects are also not yet sufficiently analyzed for a prediction.

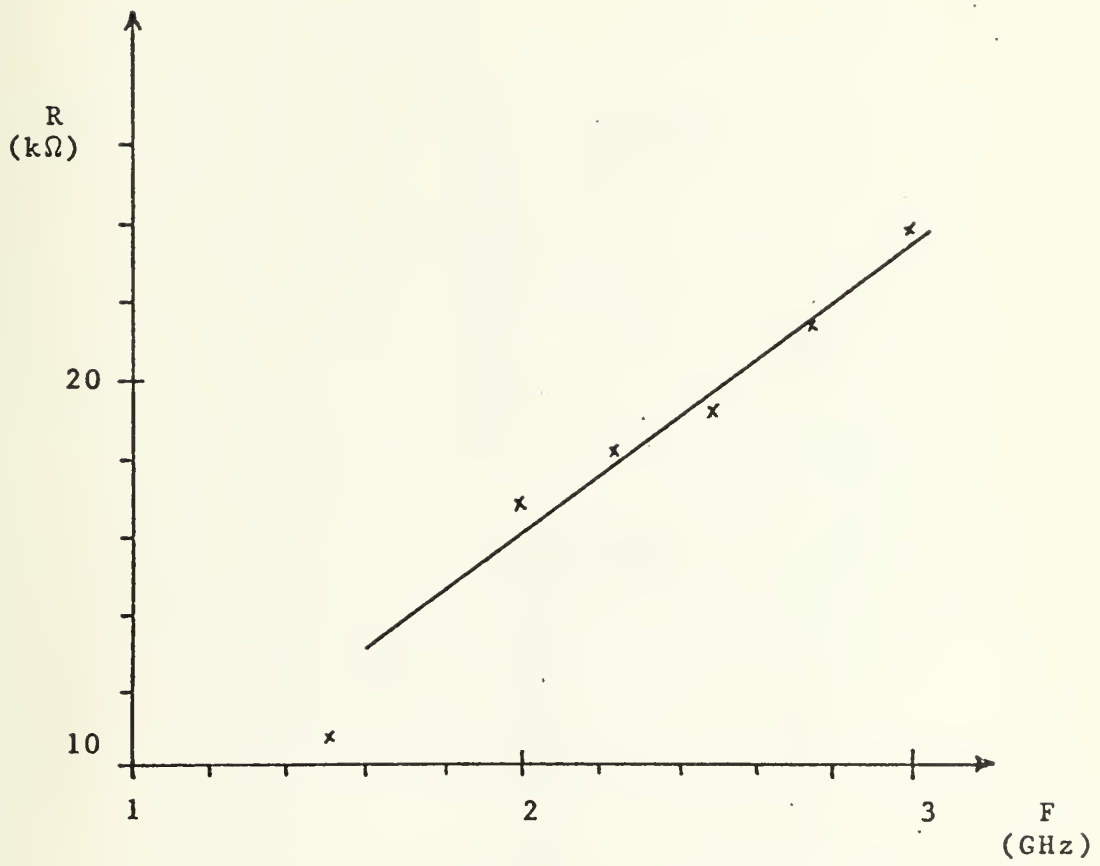

Figure 4.3/1 Resistance vs. Frequency for w/D=1, D=0.3175 cm, Dielectric Constant is 20.

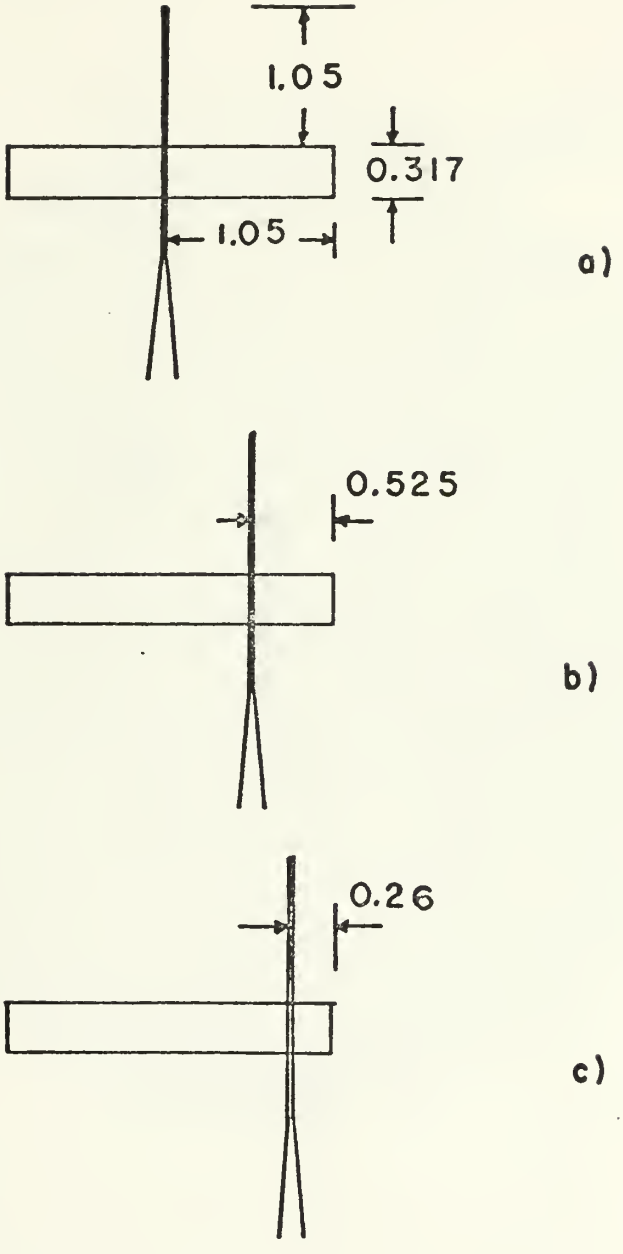

Figure 4.3/2 Positioning of the Microstrip.

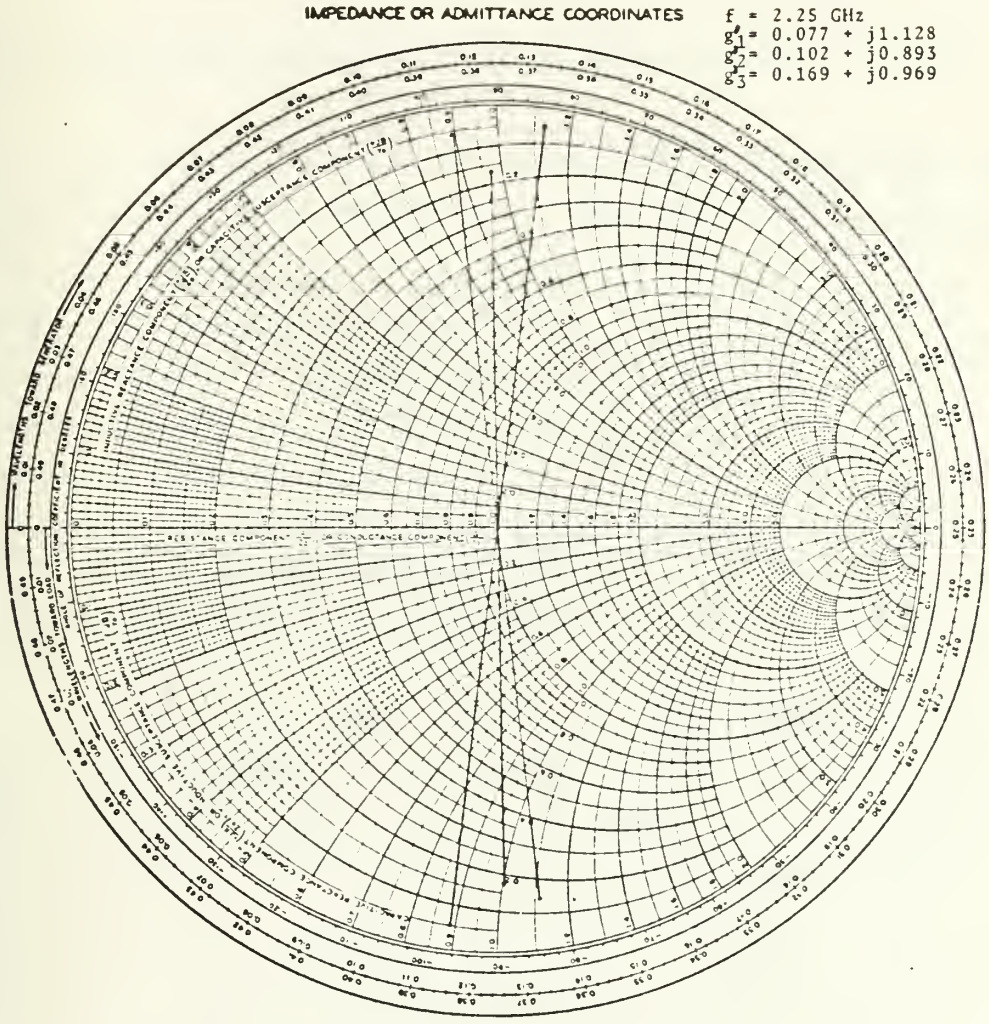

Figure 4.3/3 Input Impedance and Conductance of Three Slot Antennas with Differently Positioned Microstrips.

5. RADIATION MEASUREMENTS

After theoretical calculation of the radiation patterns and acquiring sufficient agreement between the theoretical and actual radiation resistance, radiation measurements were performed in an anechoic chamber.

5.1 SETUP FOR RADIATION MEASUREMENTS

A block diagram in figure 5.1/1 illustrates the set-up used for pattern recordings. The instruments used are:

Stable Oscillator: HP 8690 A
Frequency Meter: HP 536 A
Power Meter: HP 432 A
20dB Coupler: HP 767 D
Oscilloscope: HP 1220 A
Plotter: SA (Scientific Atlanta) Plotter
Horn Antenna: self-built
High Gain Amplifier: self-built

Because of the relative high mismatch between the impedance of the coaxial cable and the input impedance of the antenna, an isolator in front of the oscillator and a stub tuner was placed in the transmission line. As the plotter could only be driven by a 1000 Hz signal, the high frequency was modulated by it. A diode detecter in a tunable piece of waveguide detected this frequency. As the output power of the oscillator amounted to about 10 mW, it was decided, first to build a horn antenna, second to use a high gain amplifier right behind the detector stage.

The waveguide dimensions were: a = 10.9 cm, b = 5.46 cm, leading to a cut-off frequency of about 1.376 GHz. For the design of the horn antenna, the curve on page 25-37 of Ref. 6 was used for a nominal gain of 15 dB. The dimensions

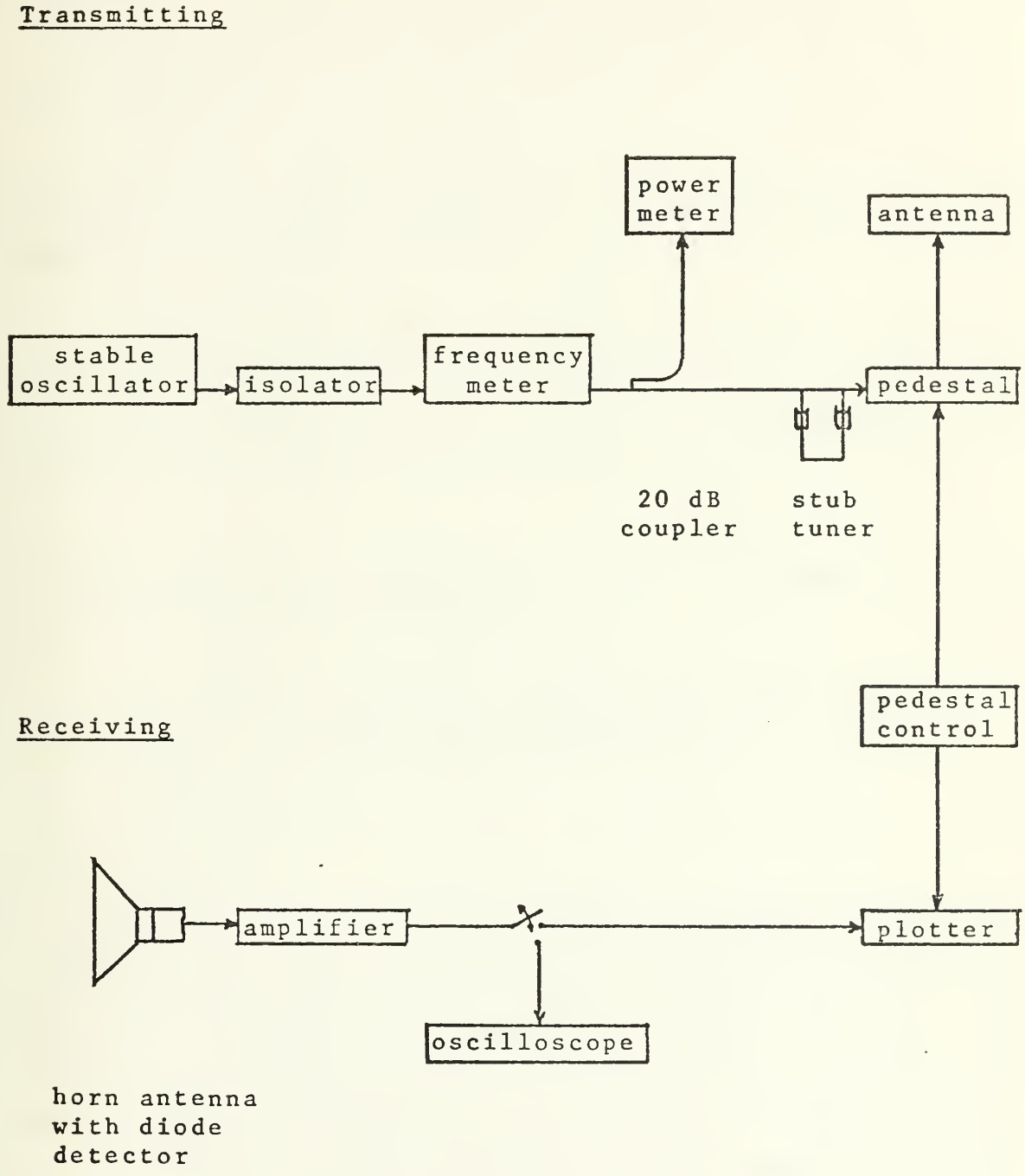

Figure 5.1/1 Setup for Pattern Recordings.

for the shortest horn length possible and a wavelength of 13.33 cm are:

A = 34 cm

B = 28 cm

L(1) = 20 cm .

The high input impedance of the plotter allowed to design the amplifier to operate on batteries in order to have it independent of a power cord.

For maximum reception, a tuning of the stub tuner and the short of the detector was essential. This could be most accurately accomplished by using an oscilloscope and connecting the plotter after tuning.

5.2 DETERMINATION OF RESONANT FREQUENCY, BANDWIDTH, AND PLOT OF THE RADIATION PATTERNS

The resonant frequencies obtained from the network analyzer in 4.3 for all three antennas are:

f(1) = 2.58 GHz

f(2) = 2.53 GHz

f(3) = 2.38 GHz

In order to measure the resonant frequencies and the bandwidth from the set-up, the stub tuner and the isolator were replaced by the circulator MODEL ON-1037 built by the Advanced Microwave Laboratories. Then a curve was constructed for each antenna. The points of these curves were obtained by measuring the received peak-to-peak voltage of the 1000 Hz modulation after the amplifier. The frequency range over which these measurements were performed was 2.0 to 2.7 GHz. All three curves are contained in figure 5.2/1. The conclusions to be drawn from these curves are:

The antenna does not only have one specific frequency at

which the radiated power peaks, but several.

The occurrence of the maximum peak and the difference to the resonant frequency obtained from the analyzer are:
Antenna 1: 2.610 GHz, difference = 0.03 GHz
Antenna 2: 2.444 GHz, difference = 0.106 GHz
Antenna 3: 2.435 GHz, difference = 0.05 GHz
The difference for antenna 2 is less if one compares the predicted resonance frequency with the third peak at 2.605 GHz which is of a slightly less magnetude. Here the difference amounts to 0.075 GHz. Thus the measured frequencies agree closely with those obtained from the microwave analyzer.

Evaluation of the 3 dB bandwidth at the maximum peak gave:
B(1) = 21 MHz
B(2) = 26 MHz
B(3) = 28 MHz

Finally a close correspondence between the curves of antenna 1 and 2 can be observed, whereas the curve of antenna 3 reveals less similarity. This feature will be recognizable again when the radiation patterns are drawn. From this fact it can be deduced that the microstrip of antenna 3 reaches in the edge effect region of the slot.

What remains to be answered is the question for the cause of the several peaks. The explanation lies in the behaviour of the microstrip which does not present a constant input impedance for different frequencies.

After finding the resonant frequency by experiment, the three antennas were tuned to this frequency for recording the radiation patterns. The vertical and horizontal patterns obtained with the set-up are drawn in figure 5.2/2 and 5.2/3 respectively. These patterns are quite different from what theory predicted in the figures 2.4/1 and 2.4/2.

The free space wavelength for the used frequency, however, is about 13.33 cm. Thus assumption 2.1a would demand a board with dimensions of about ten wavelengths on one side of the board to be valid, i.e. at least a square meter board should be used. Due to the costs of copper coated dielectric plates, a board of a side-length of 7.5 cm was constructed which does not justify the above assumption. The good approximation of the theoretical patterns,however, could roughly be indicated by measuring the received voltage at a radiating angle of ten degrees in two ways: first without any additional device, second with a metal plate placed in the extension of the board as a rough approximation of a larger sized board. For the vertical pattern the received voltage dropped to about 15 percent of its previous value, indicating the null ten degrees further of the pattern in figure 2.4/1. When performing the same experiment for the horizontal pattern, an increase of the voltage to almost the maximum value was observable. Though being an inaccurate means, it indicates the direction of change and the validity of the theoretical calculations. As mentioned above, the patterns of antenna 1 and 2 are very similar, whereas the pattern of antenna 3 reveals the intrusion of the microstip into the edge effect region of the slot.

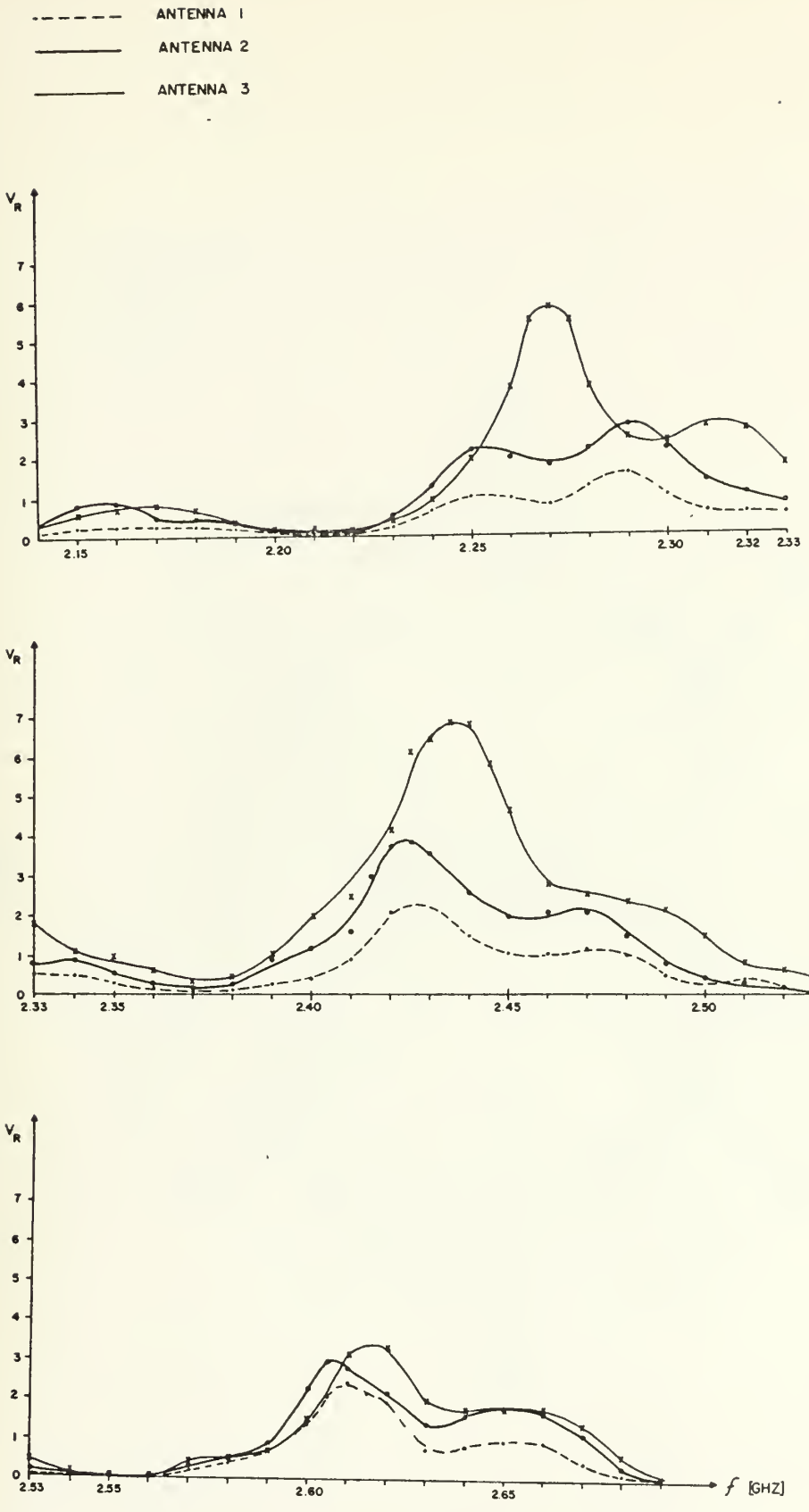

Figure 5.2/1 Signal Strength vs. Frequency.

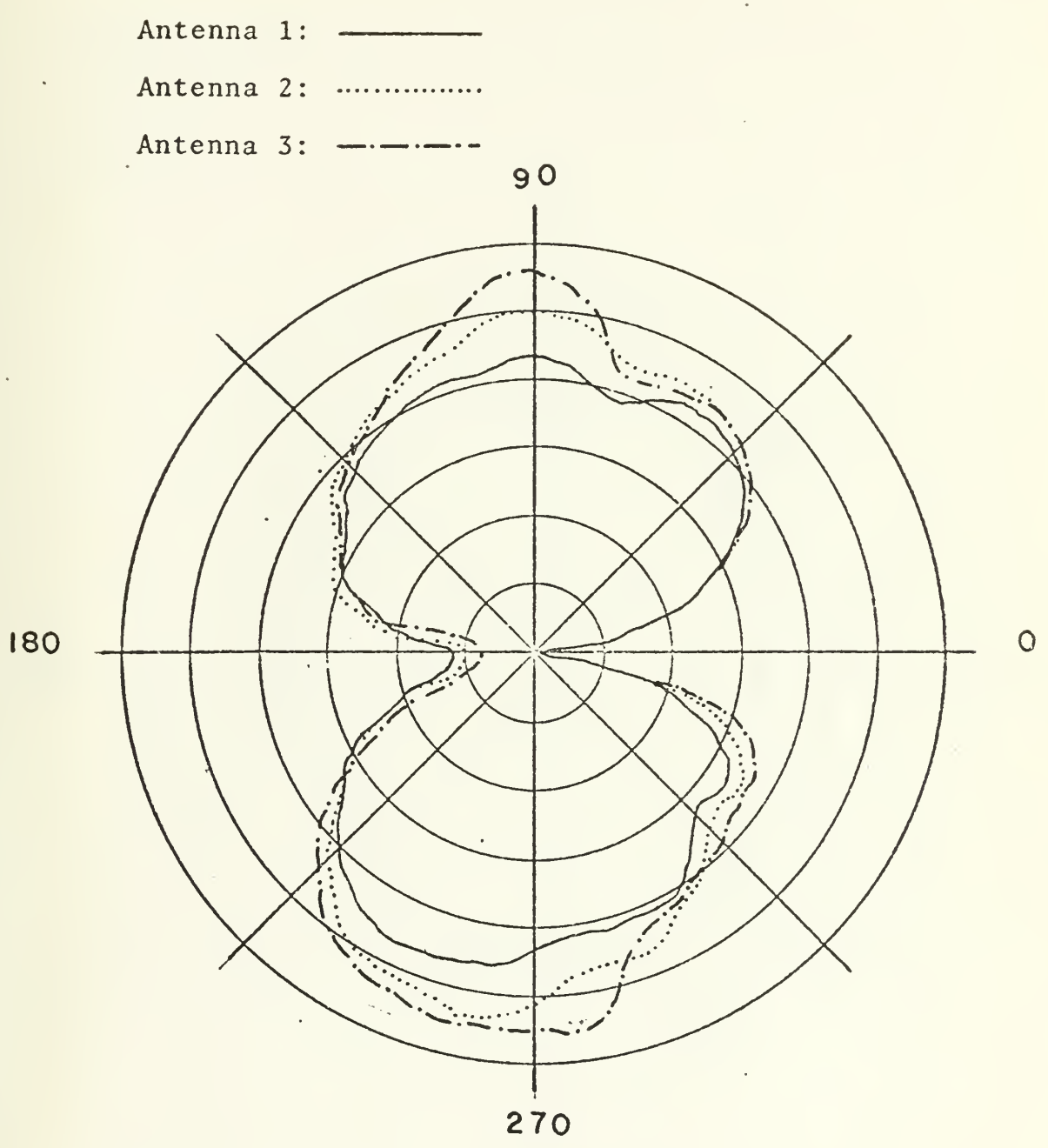

Figure 5.2/2 Radiation Pattern in the Vertical Plane.

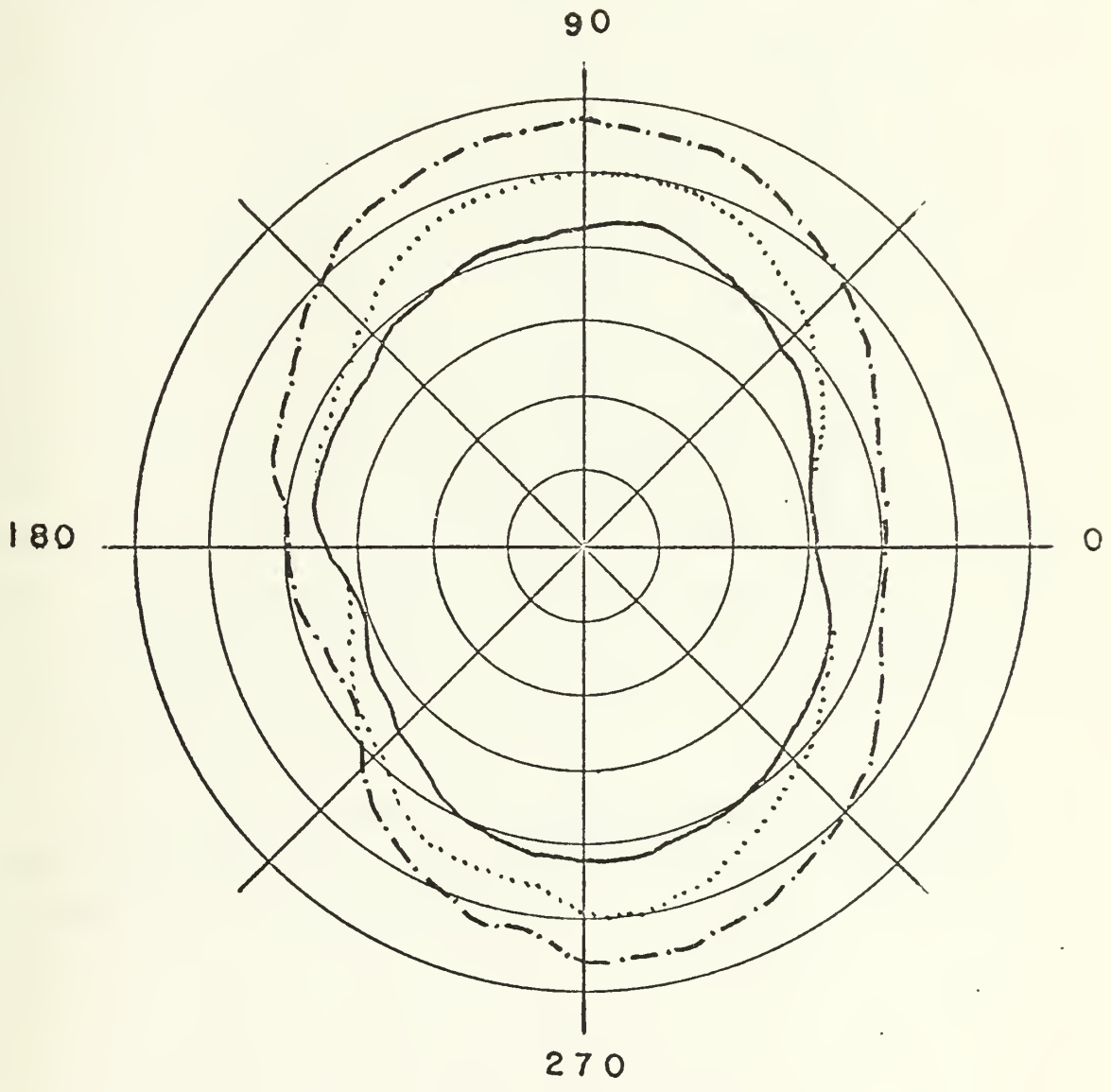

Figure 5.2/3 Radiation Pattern in the Horizontal Plane.

6. SUMMARY AND CONCLUSION

Radiation resistance and patterns of a dielectric backed slot antenna were studied in theory and practice. Agreement with both methods was achieved. The similarity between a dipole and a slot antenna is especially perceptible in the radiation patterns. The radiation resistance, however, was found to be almost two orders of magnetude higher. This lead to considerations about changing the transition from the coaxial cable to the slot, in order to have a lower reflection coefficient. Two methods were used, tapering the microstrip and positioning it differently with respect to the slot. The effect of the last method can roughly be predicted, the precision of which depending on the distance of the microstrip to the edge of the slot. As long as the region is not reached where the edge effects are important, the radiation pattern and the form of the curve signal strength vs. frequency does not change. The transition, however, causes the antenna to reach maximum radiation at several frequencies, not only at the predictable resonance frequency. The 3 dB bandwidth at these maxima is about equal and a little more than one percent of the center frequency.

In order to reduce the radiation resistance, one would have to use lower frequencies as the resistance is proportional to the frequency.

7. SUGGESTIONS FOR FURTHER STUDIES

Though the main features of a dielectric backed slot antenna were studied, several problems remain for further investigation.

The main topics are an examination and analysis of the edge effects of the slot and the radiation from the backside of the board. A mathematical analysis, however, is thought to be of great complexity.

Also the application of resonant slots for radiating into a waveguide may be subject to a study.

APPENDIX A

CALCULATOR PROGRAM 1

```
0:
ENT  "MIN,MAX:X,Y",R31,R32,R33,R34;FLT 4
1:
ENT "AXES?",R43;IF R43=0;GTO "PLOT"
2:
ENT "0 CROSS:X,Y",R35,R36,"NTICS"X,Y",R37,R38,
"TITLE:X,Y",R39,R40
3:
SCL R31,R32,R33,R34;(R32-R31)/R37→R41;(R34-R33/ R38→R42
4:
AXE R35,R36,R41,R42
5:
.03175→R0;1.0→R1;.384→R2;.358→R3
6:
3.14*R0*R1→R4;3.14*R2*R3→R5;2/3.14*R5→R6
7:
0→R7;3.14/180→R8;0→R9;3.14/180→R10;TBL 2
8:
ENT "THETA",R7,"PHI",R9,"L",R14
9:
"GO";R4*SIN R7*COS (R5*COS R7) →R11
10:
(R6*COS R7)↑2-1→R12
11:
-R14*2000/9.86R12→R15
12:
R15*COS R7→X;R15*SIN R7→Y
13:
PLT X,Y
14:
R7+R8→R7;IF R7≤3.14;GTO "GO"
15:
LTR .80R32,.15R33,311;PLT "THETA"
16:
FXD 1;LTR R39,R40,421;PLT "E VS THETA,PHI " FXD 1;LTR
R39,R40,421;PLT "E VS THETA,PHI IS ";PLT R9
17:
END
```

APPENDIX B

CALCULATOR PROGRAM 2

```
0:
ENT  "MIN,MAX:X,Y",R31,R32,R33,R34;FLT 4
1:
ENT "AXES?",R43;IF R43=0;GTO "PLOT"
2:
ENT "0 CROSS:X,Y",R35,R36,"NTICS"X,Y",R37,R38,
"TITLE:X,Y",R39,R40
3:
SCL R31,R32,R33,R34;(R32-R31)/R37→R41;(R34-R33/ R38→R42
4:
AXE R35,R36,R41,R42
5:
.03175→R0;1.0→R1;.384→R2;.358→R3
6:
3.14*R0*R1→R4;3.14*R2*R3→R5;2/3.14*R5→R6
7:
0→R7;3.14/180→R8;0→R9;3.14/180→R10;TBL 2
8:
ENT "THETA",R7,"PHI",R9,"L",R14
9:
"GO";SIN (R4*COS R9*SIN R7)*COS (R5*COS R7)→R11
10:
COS R9*((R6*COS R7)↑2-1)→R12
11:
-R14*R11*200C/9.86R12→R15
12:
R15*COS R7→X;R15*SIN R7→Y
13:
PLT X,Y
14:
R7+R8→R7;IF R7≤3.14;GTO "GO"
15:
LTR .80R32,.15R33,311;PLT "THETA"
16:
FXD 4;LTR R39,R40,421;PLT "E VS THETA,PHI IS ";PLT R9
17:
END
```

APPENDIX C

CALCULATOR PROGRAM 3

```
0:
ENT  "MIN,MAX:X,Y",R31,R32,R33,R34;FLT 4
1:
ENT "AXES?",R43;IF R43=0;GTO "PLOT"
2:
ENT "0 CROSS:X,Y",R35,R36,"NTICS"X,Y",R37,R38,
"TITLE:X,Y",R39,R40
3:
SCL R31,R32,R33,R34;(R32-R31)/R37→R41;(R34-R33/ R38→R42
4:
AXE R35,R36,R41,R42
5:
.01375→R0;1.0→R1;.384→R2;.358→R3
6:
3.14*R0*R1→R4;3.14*R2*R3→R5;2/3.14*R5→R6
7:
0→R7;3.14/180→R8;0→R9;3.14/170→R10;TBL 2
8:
ENT "THETA",R7,"PHI",R9,"L",R14
9:
"GO";SIN (R4*COS R9*SIN R7)*COS (R5*COS R7)→R11
10:
COS R9*((R6*COS R7)↑2-1)→R12
11:
-R14*R11*2000/9.86R12→R15
12:
R15*COS R9→X;R15*SIN R9→Y
13:
PLT X,Y
14:
R9+R10→R9;IF R9≤3.14;GTO "GO"
15:
LTR .80R32,.15R33,311;PLT "PHI"
16:
FXD 4;LTR R39,R40,421;PLT "E VS PHI,THETA IS ";PLT R7
17:
END
```

APPENDIX D

PROGRAM FOR NUMERICAL INTEGRATION

```
   10 FORMAT (' THE NUMERICAL APPROXIMATION IS:    ',E13.5)
C    SPECIFY CONSTANTS
       DOL1=0.03175
       WOD=1.0
       L2OL1=0.358
       LOL2=0.379
       PHI=4.0*ATAN(1.0)
       C1=PHI*DOL1*WOD
       C2=PHI*LOL2*L2OL1
       C3=(2.0/PHI)*C2
       I=200
       XI=200.0
       J=200
       FSUM=0.0
       XRMT=PHI/XI
       X2=XRMT/2.0
C    CALCULATE AREA
       DO 110 K=1,I
       DO 100 L=1,J
       F=(SIN(K*XRMT-X2)*(SIN(C1*COS(L*XRMT-X2)
      1*SIN(K*XRMT-X2)))**2*(COS(C2*COS(K*XRMT-X2)))**2)/
      2(COS(L*XRMT-X2)**2*((C3*COS(K*XRMT-X2))**2-1.0)**2)
       FSUM=FSUM+F
  100 CONTINUE
  110 CONTINUE
       FSUM=FSUM*(XRMT**2)
       WRITE (6,10) FSUM
       STOP
       END
```

LIST OF REFERENCES

1. Jordan, E.C. and Balman, K.G., Electromagnetic Waves and Radiating Systems, 2d ed., Prentice-Hall, Inc., 1968.

2. Mariani, E.A., Heinzman, C.P., Agrios, J.P. and Cohn, S.B., "Slot Line Characteristics", IEEE Trans. Microwave Theory Techn. (1969 Symposium Issue), vol. MTT-21 pp. 579-580, September 1969.

3. Knorr, J.B. and Saenz, J., "End Effects in a Shorted Slot", IEEE Trans. Microwave Theory Techn., vol. MTT-21 pp. 579-580, September 1973.

4. Knorr, J.B., Microwave Stripline Circuit Fabrication, paper presented as a laboratory handout at the US Naval Postgraduate School, Monterey, Calf., 1973.

5. Knorr, J.B., "Slot Line Transitions", IEEE Trans. Microwave Theory Techn., vol. MTT-22 pp. 548-554, May 1974.

6. Reference Data for Radio Engineers, 5th ed., International Telephone and Telegraph Corporation, 1973.

INITIAL DISTRIBUTION LIST

		No. Copies
1.	Defense Documentation Center Cameron Station Alexandria, Virginia 22314	2
2.	Library, Code 0212 Naval Postgraduate School Monterey, California 93940	2
3.	Department Chairman, Code 52 Department of Electrical Engineering Naval Postgraduate School Monterey, California 93940	2
4.	Assoc. Professor J. B. Knorr, code 52Ko Department of Electrical Engineering Naval Postgraduate School Monterey, California 93940	1
5.	Marineamt - AL - 294 Wilhelmshaven Federal Republic of Germany	1
6.	Dokumentationszentrale der Bundeswehr (See) 53 Bonn Friedrich-Ebert-Allee 34 Federal Republic of Germany	1
7.	LCDR U. S. Kahre, FGN Kdo Marineführungssysteme 294 Wilhelmshaven Federal Republic of Germany	2

Thesis
K1077
c.1

Kahre

A study of a dielectric backed resonant slot antenna.